# A COMPUTATIONALLY EFFICIENT MODEL FOR THREE-DIMENSIONAL STRESS ANALYSIS OF STIFFENED CURVED PANELS

Mayank Patni[1], Sergio Minera[2], Paul M. Weaver[3] and Alberto Pirrera[4]

[1] Research Assistant, mayank.patni@bristol.ac.uk
[2] Research Assistant, sergio.minera@bristol.ac.uk
[3] Professor in Lightweight Structures, paul.weaver@bristol.ac.uk
[4] Senior Lecturer in Composite Structures, alberto.pirrera@bristol.ac.uk

Bristol Composites Institute (ACCIS), University of Bristol, University Walk, Bristol BS8 1TR, UK

**Keywords:** stiffened panel, 3D stress field, unified formulation, curved section, mapping technique

**ABSTRACT**

**Lightweight, thin-walled structures stiffened by a set of stringers or ribs are widely used in many engineering applications. Thus, the need for the structural capability assessment of such structures has increased and development of accurate, yet computationally efficient, models has become a major interest to industry. We present a novel approach for the static analysis of stiffened structures using a one-dimensional (1D) refined beam model. The approach is based on Carrera Unified Formulation (CUF), and can recover complex, three-dimensional (3D) stress fields in a computationally efficient manner. As a novelty, recently developed hierarchical set of expansion functions, based on Lagrange polynomials, namely Serendipity Lagrange expansions (SLE), are used to define cross-sectional displacements. In this scheme, the beam's cross-section is discretised using four-node Lagrange elements, which allows local stress-concentrations to be modelled. Further, the hierarchical nature of Serendipity Lagrange expansions within each cross-sectional element make it suitable for predicting higher-order effects. The higher-order expansion functions also improve the geometrical approximation of curved sections by employing a local mapping technique based on a blending function method. In the present work, the so-called 1D CUF-SLE model is used to analyse flat and curved panels stiffened with transverse ribs and longitudinal stringers. The performance of the proposed approach in terms of computational cost and precision is assessed in comparison to reference solutions obtained by employing 3D finite element (FE) analysis in ANSYS. Our results show the capability of the present formulation to model complex structures which otherwise could only be done with computationally expensive 3D FE analysis.**

## 1 INTRODUCTION

Stiffened structures are extensively used in many engineering fields, namely the aerospace, automobile, naval and civil engineering industries. The reason is due to their high strength-to-weight ratio, which is obtained by reinforcing thin-walled shells with a set of stiffeners, either transversal ribs or longitudinal stringers. Further, composite materials add significant value to these structures' application. Therefore, determination of accurate stress/strains in stiffened composite components is of prime interest for structural analysts. Researchers have proposed various models and techniques to analyse the static response of these structures. The simplest approach to studying a stiffened panel is replacing it with an equivalent orthotropic plate of constant thickness, obtained by smearing-out the stiffness property of ribs (or stiffeners) over the plate [1]. However, this method generally leads to erroneous results if the stiffeners are not closely spaced. Another approach is employing a discrete analysis technique, where the plate and the stiffeners are modelled separately while maintaining continuity of displacements and forces at the interface [2]. A similar method was proposed where the portion of a skin between the stiffeners are modelled, assuming the edges as simply-supported or

clamped, and several closed-form solutions are available for isotropic and composite materials [3, 4]. Despite various analytical and semi-analytical methods, only a few of them allow flat and curved composite panels to be studied under combined loading conditions and therefore, more emphasis is being laid on numerical techniques using energy principles, the finite element method, constraint method and boundary element method [5]. Out of these, the finite element method (FEM) is widely adopted as a design and analysis tool in many industries. However, the accuracy of the solution obtained depends upon the type of element used. Discretising the reinforced structure with a finite number of three-dimensional (3D) or solid elements, yields precise results as their kinematics is not afflicted by fundamental assumptions. But this requires calculation of a large number of unknowns which leads to high computational cost. In contrast, using 1D elements (for stringers) and 2D elements (for the panel) can be economical but the accuracy of the solution is not guaranteed. As these elements are based on classical structural theories, they are unable to capture non-classical effects like severe transverse shear deformations and are only applicable to regions remote from boundary constraints, discontinuities and points of load application. The errors get further compounded when employed for composite plates due to the low ratio of transverse shear stiffness to bending stiffness. This effect will exacerbate in stiffened composite structures and have been the focus of attention in several papers [6, 7, 8].

To develop a benchmark solution that captures non-classical phenomena in stiffened plates and predicts 3D stress fields accurately, it is required to rigorously model the plate and stiffeners with 3D solid elements. However, these models are computationally expensive when used for laminates with a large number of layers, in optimization studies, or for non-linear analyses. Hence, there is a need to develop a simpler model which rules out the requirement for a complete 3D analysis of the stiffener and yet accurately captures non-classical effects in stiffened structures.

The use of refined structural theories can be an alternative to classical approaches and is able to provide accurate solutions [9]. Of relevance to the present work, one of the most recent contributions to the development of refined beam theories is the Unified Formulation by Carrera and co-workers [10, 11]. The formulation provides 1D (beam) and 2D (plate and shell) models that go beyond the classical approximations by exploiting a compact, hierarchical notation that allows most classic and recent formulations to be retrieved from one, hence *unified*, model. The displacement field is expressed over the cross-section (beam case) and through the thickness (plate and shell cases) by employing various expansion functions including Taylor (TE) polynomials, Lagrange (LE) polynomials, exponential and trigonometric functions, Chebyshev and Legendre polynomials. Amongst these, TE and LE models are most widely adopted. The recently developed Serendipity Lagrange expansion (SLE) model is found to solve some of the shortcomings of these commonly used Carrera Unified Formulation (CUF) beam models [12]. The SLE model combines two of the main features of TE and LE models, i.e. it is hierarchical and allows for numerically stable cross-sectional refinements via remeshing. With the hierarchical approach, it is easy to build higher-order models which further helps in the correct mapping of curved sections.

In this work, a 1D CUF-SLE model, derived and assessed in the previous work [12], is used for the analysis of stiffened flat panel. The results are compared with those obtained by 3D finite element analysis performed in a commercial code, ANSYS. Further, existing model capabilities are extended by employing a higher-order mapping technique, based on blending functions, to describe curved sections. To the authors' knowledge, this enhanced model is used for the first time in the literature to compute 3D stress fields in a curved stiffened panel.

The remainder of the paper is structured as follows. Section 2 provides an overview of 1D Carrera Unified Formulation based on Serendipity Lagrange expansions. Section 3 presents a brief summary of the mapping techniques employed herein for analysing curved cross-sections. Numerical results obtained for flat and curved panels are found in Section 4. Finally, conclusions are drawn in Section 5.

## 2 ONE-DIMENSIONAL UNIFIED FORMULATION

CUF relies on a displacement-based formulation of the finite element method. In this setting, the 3D displacement field is given as

$$\boldsymbol{U}(x,y,z) = \begin{Bmatrix} u_x(x,y,z) \\ u_y(x,y,z) \\ u_z(x,y,z) \end{Bmatrix}. \tag{1}$$

To overcome the limitations of classical beam models and to predict displacement fields more accurately, one typical way is to enrich the kinematics. In CUF, refined beam models with an arbitrary number of terms in the kinematic field can be readily developed. Consider a beam-like structure, where the beam extends along *y*-axis and cross-section lie in the *xz*-plane. The displacement field $\boldsymbol{U}(x,y,z)$ is written as a product of two functions: cross-section expansion functions, $F(x,z)$, and 1D Lagrange shape functions, $N(y)$, along the beam axis. In principle, these functions can have as many terms as desired. The more the terms, the richer the kinematics. In the current formulation, the beam is discretised along the length with traditional 1D finite elements and cross-sectional deformations are approximated using SLE functions as explained in Section 2.1. Mathematically, this means that the displacement field and its variation can be written as

$$\begin{aligned} U &= F_\tau(x,z)N_i(y)u_{i\tau}\,, \\ \delta U &= F_s(x,z)N_j(y)\delta u_{js}\,, \end{aligned} \tag{2}$$

with $\tau, s = 1,\dots,m$, where $m$ is the number of terms that depends on the order of expansion; $i,j = 1,\dots,N_{NE}$, with $N_{NE}$ being the number of nodes per element; and finally, $u_{i\tau}$ and $u_{js}$ are the generalised displacement vectors.

The governing equations are derived using the Principle of Virtual Displacements (PVD) in the static formulation

$$\delta W_{int} = \delta W_{ext}\,, \tag{3}$$

where $\delta$ denotes virtual variation with respect to the displacements, and $W_{int}$ and $W_{ext}$ denote internal and external work, respectively.

The internal work can be written as

$$\delta W_{int} = \int_l \int_\Omega \delta\varepsilon^T \sigma \, d\Omega dl\,, \tag{4}$$

where $l$ is the length of the beam and $\Omega$ represents the surface of the cross-section domain. By considering the kinematic field as given by equation (2) and the 3D constitutive and geometrical relations [10], the expression of the internal work can be rewritten as

$$\delta W_{int} = \delta u_{js}^T \boldsymbol{K}^{\tau sij} u_{i\tau}\,, \tag{5}$$

where $\boldsymbol{K}^{\tau sij}$ represents the 3 x 3 fundamental nucleus of the element stiffness matrix, derived assuming small displacements and strains, in the present work. It is to be noted that the final expression of the fundamental nucleus is invariant of the choice of expansion polynomials and beam shape functions. Fundamental nuclei are assembled in a global stiffness matrix following the standard finite element procedure. A detailed description of 1D formulations based on CUF can be found in [10, 11].

### 2.1 Serendipity Lagrange Expansion model

The SLE model is derived by adopting a hierarchical set of Lagrange-type polynomials to expand the generalised displacement variables over the cross-section. In this model, cross-sections are discretised using four-node Lagrange sub-domains and the displacement field within the sub-domains can be enriched by increasing the order of local Serendipity Lagrange expansion. Each physical sub-domain is

mapped into a natural reference system as shown in Figure 1. Three different sets of 2D-polynomials are required to define the cross-section expansion functions.

- Polynomials of type I: These are the same as linear Lagrange polynomials, defined to satisfy vertex continuity.

$$F_\tau^I = \frac{1}{4}(1+\xi_s\xi)(1+\eta_s\eta) \qquad \tau = 1,2,3,4, \tag{6}$$

where $(\xi_s, \eta_s)$ are coordinates of the four corner nodes of sub-domain in the natural reference system.

- Polynomials of type II: These are defined to satisfy the continuity of displacements across cross-sectional sub-domains, i.e. side continuity.

$$\begin{aligned} F_\tau^{II} &= \frac{1}{4}(1-\eta)p_r(\xi) \qquad \tau = 5,9,13,18,\dots \\ F_\tau^{II} &= \frac{1}{4}(1+\xi)p_r(\eta) \qquad \tau = 6,10,14,19,\dots \\ F_\tau^{II} &= \frac{1}{4}(1+\eta)p_r(-\xi) \qquad \tau = 7,11,15,20,\dots \\ F_\tau^{II} &= \frac{1}{4}(1-\xi)p_r(\eta) \qquad \tau = 8,12,16,21,\dots \end{aligned} \tag{7}$$

where $p_r$ corresponds to the 1D Lagrange-type polynomials as given in [13].

- Polynomials of type III: These are defined in the interior subset, also called internal expansions and are included for order, $N \geq 4$. In total, there are $(N-2)(N-3)/2$ internal polynomials given by

$$F_\tau^{III} = p_n(\xi)p_m(\eta) \qquad \tau = 17,22,23,\dots \tag{8}$$

with $n, m = 2,3,\dots,N$ and constrained by $n+m=r$ and $n+m \leq N$, where $r = 1,2,\dots,N$. The reader is referred to [12] for more detailed treatment of SLE models.

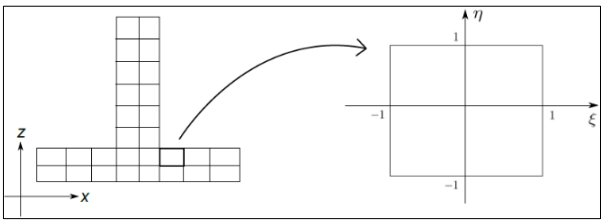


Figure 1: Mapping from physical sub-domain to natural reference system

## 3 CROSS-SECTION MAPPING

A correct geometrical description of the structure is of fundamental importance when dealing with complex geometries and curved section beams. The SL expansion functions, as defined in the previous section, are used to enrich the kinematics in the cross-section. These functions are integrated over the cross-section of the beam, which requires transformation of the coordinates. If the edges of a quadrilateral element are straight, the approximation of the geometry is obtained through linear mapping by using linear Lagrange polynomials. However, to represent curved edges, higher-order polynomials can be used [14]. In this paper, since the geometries analysed are represented by circular arcs, a non-linear function representing equation of a circle is employed. The choice of this function guarantees the exact description of shape, normal and tangents at each point on the curve, unlike using higher-order polynomials which can lead to numerical errors due to approximation.

To understand the procedure, consider a section as shown in Figure 2(a) which is discretised using quadrilateral domains. In each domain, two of the sides are curved and the coordinates of these sides are represented by

$$\begin{aligned} x &= x_{c1}(\xi) + x_{c2}(\xi), \\ z &= z_{c1}(\xi) + z_{c2}(\xi), \end{aligned} \tag{9}$$

where $x_{c1}(\xi), z_{c1}(\xi)$ and $x_{c2}(\xi), z_{c2}(\xi)$ are functions, as given below, that represents the curved edges with radius of curvature $r_1$and $r_2$.

$$\begin{aligned} x_{c1}(\xi) &= \frac{1}{2}(1-\xi)x_1 + \frac{1}{2}(1+\xi)x_2, \\ x_{c2}(\xi) &= \frac{1}{2}(1+\xi)x_3 + \frac{1}{2}(1-\xi)x_4, \\ z_{c1}(\xi) &= \sqrt{(r_1^2 - x_{c1}^2)}, \\ z_{c2}(\xi) &= \sqrt{(r_2^2 - x_{c2}^2)}, \end{aligned} \tag{10}$$

where $x_1, x_2, x_3, x_4$ are the *x*-coordinates of the corners of a quadrilateral element as shown in Figure *2*(b). These functions are defined in such a way that $x_{c1}(-1) = x_1$ and $x_{c1}(1) = x_2$. Similarly, $x_{c2}(-1) = x_3$ and $x_{c2}(1) = x_4$. Applying the blending function method, the mapping functions are written as

$$\begin{aligned} x &= \frac{1}{2}(1-\eta)x_{c1} + \frac{1}{2}(1+\eta)x_{c2}, \\ z &= \frac{1}{2}(1-\eta)z_{c1} + \frac{1}{2}(1+\eta)z_{c2}. \end{aligned} \tag{10}$$

This procedure can be expanded to all the edges in case of a quadrilateral domain with all sides curved.

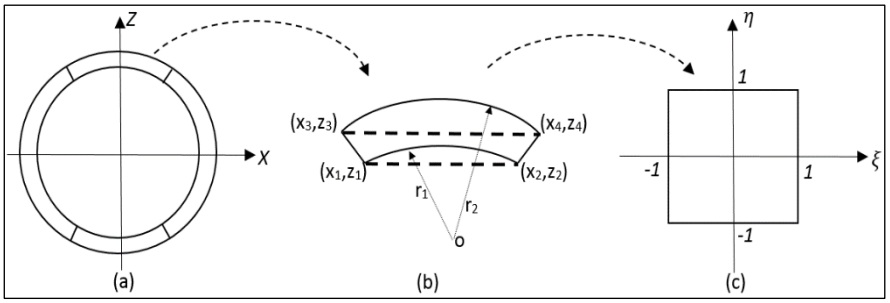


Figure 2: Mapping curved element

## 4 NUMERICAL RESULTS

This section aims to investigate the behaviour of previously introduced 1D CUF, based on SLE model, in the analysis of stiffened structures. The first part of this work presents the static analysis of a flat panel with stiffeners reinforced in longitudinal and transverse directions. In the second part, a similar but curved panel is used to assess the validity of the mapping techniques employed on the SLE model for analyzing curved cross-section geometries. These examples have been selected to show the capabilities of the present formulation in representing a wide range of structures used in civil and aerospace industries. The present formulation requires these structures to be modelled as a 1D beam with different cross-sections running along the length. To understand this modelling strategy, consider two beam models, beam-A and beam-B. Beam-A represents the panel reinforced with longitudinal stringers, with the beam axis aligned along its length and cross-section as shown in Figure 3(a) and 4(a) for flat and curved panels, respectively. While beam-B represents the panel reinforced with a transverse stiffener, with beam axis aligned along the thickness direction and the section normal to it is treated as its cross-section as shown in Figure 3(b) for flat and Figure 4(b) for curved. These beam models are connected along the length to get the desired structures. The cross-section discretisation feature of SLE model within the CUF framework allows different cross-section beams to connect and maintain the displacement continuity at the interface.

All the essential geometrical parameters for stiffened flat and curved panels, considered in the present study, are described in Figure 3 and Figure 4. The constituent material is isotropic with Young's

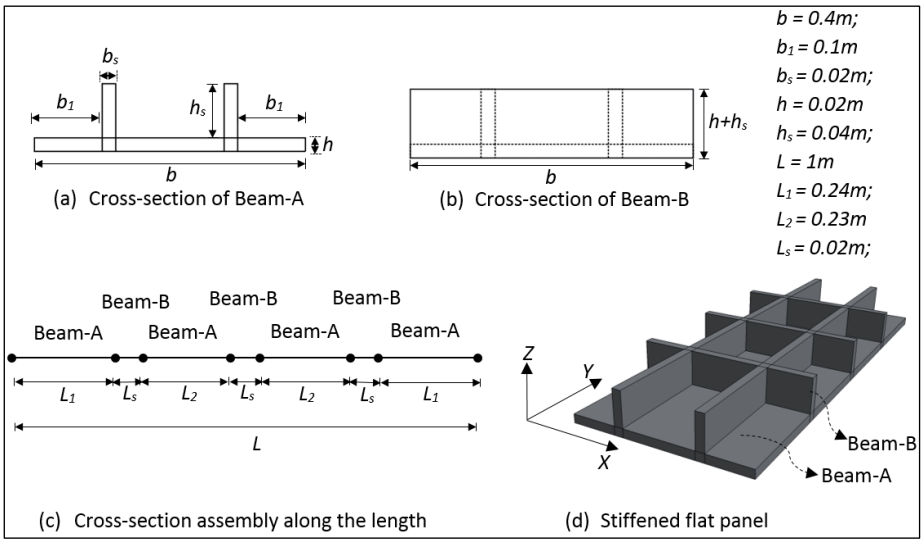


Figure 3: Stiffened flat panel – Geometry

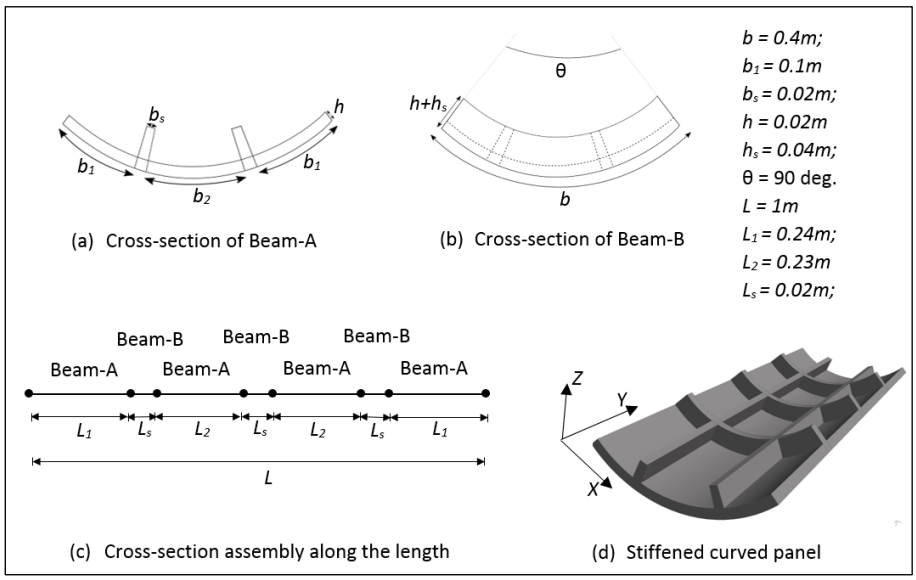


Figure 4: Stiffened curved panel - Geometry

modulus $E = 71.7$ GPa and Poisson's ratio $\nu = 0.3$. The structures are clamped at one end ($y = 0$) and a surface load of 1 kN is applied across the section at the other end ($y = 1$ m). The load applied in case of a flat panel is in the negative *z*-direction, whereas in case of a curved panel it is in the positive *z*-direction. For both cases, beam-A and beam-B are discretised using five- and three-B4 (four-node cubic) elements, respectively, which adds up to 29 B4 elements in the complete structure. It is to be noted that the distribution of nodes, within each beam subset, follows the Chebyshev distribution, as given in [12]. In doing so, the accuracy of the results is increased near the stringer-rib interface as well as towards the clamped end, without the need to increase the total number of beam nodes. Further, the cross-sections of beam-A and beam-B are discretised with twenty-two and forty-two SL5 (four-node Serendipity Lagrange element with fifth-order expansion). This results into 110,220 unknown variables or degrees of freedom (DOFs). The number of beam elements, cross-sectional mesh and the order of expansion is decided by performing a convergence analysis. For the sake of brevity, only the converged results for all the cases are presented in the paper. In both the numerical cases assessed, stresses are computed at various locations along the beam and are compared with those obtained with high fidelity 3D finite element analyses.

### 4.1 Stiffened flat panel

Results obtained by performing the static analysis of a stiffened flat panel are presented in this section. To validate the present approach, a reference solution is required, which is obtained by discretising the structure with a finite number of 3D elements and analysing it using commercial finite element package, ANSYS. A mesh convergence analysis is performed which ensures that an optimum number of elements are employed to obtain accurate results. In this case, the model is discretised with 669,696 SOLID186 (3D 20-node) elements, which leads to solving 8,832,243 equations (DOFs).

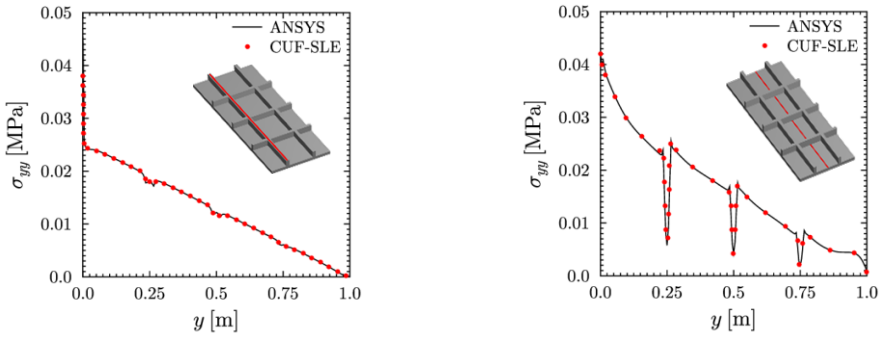


(a) $\sigma_{yy}$ for $(x, z) = (b_1 + b_s/2, h + h_s)$ and $y \in [0, L]$ (b) $\sigma_{yy}$ for $(x, z) = (b/2, h)$ and $y \in [0, L]$

Figure 5: Variation of axial normal stress ($\sigma_{yy}$) along the length of the flat panel.

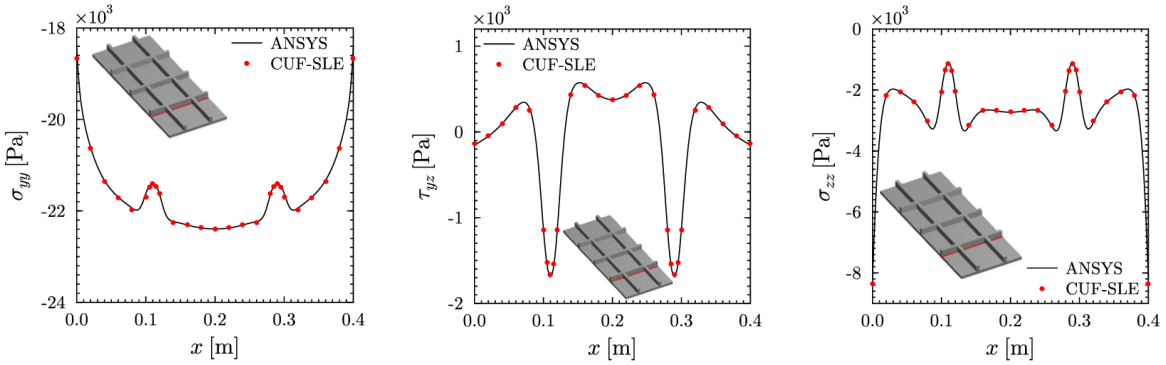


(a) Axial normal stress ($\sigma_{yy}$) (b) Transverse shear stress ($\tau_{yz}$) (c) Transverse normal stress ($\sigma_{zz}$)

Figure 6: Variation of normal and shear stresses across the panel width at $(y, z) = (L/4, h/2)$.

Normal stress ($\sigma_{yy}$) values are plotted along the length of the panel at two different locations as shown in Figure 5. These results are key towards the validation of the present modelling technique of connecting different cross-sections along the beam length. This displacement-based formulation naturally satisfies the displacement continuity requirement at the stringer-rib interface; however, a higher-order displacement field approximation is required to obtain a continuous stress/strain distribution. The present model clearly meets this requirement and hence no discrepancies are observed in the normal stress values along the length when compared to those obtained with ANSYS.

Further, to demonstrate the capability of the proposed model in predicting the 3D stress fields in such structures, normal and transverse stress components have been measured at several locations. The distribution of axial normal ($\sigma_{yy}$), transverse shear ($\tau_{yz}$) and transverse normal ($\sigma_{zz}$) stresses are plotted, along the width of the panel at $(y, z) = (L/4, h/2)$ in Figure 6 and through-thickness at $(x, y) = (b/2, L/4)$ in Figure 7. To show the ability of the model in capturing the accurate structural response particularly at the rib-stringer junction, through-thickness normal and transverse stresses are presented in Figure 8. All these plots clearly show that the stress values are in excellent agreement with those obtained with ANSYS. In addition, the proposed higher-order refined beam model can capture 3D stress fields accurately in a computationally efficient manner.

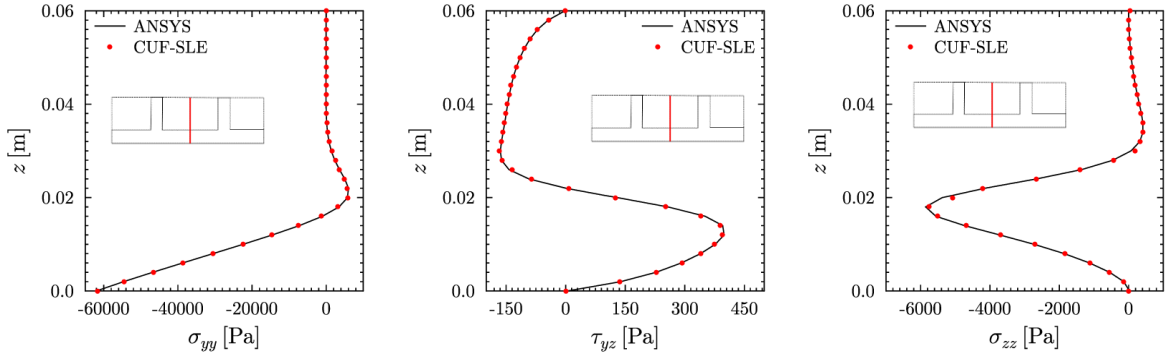


(a) Axial normal stress ($\sigma_{yy}$) (b) Transverse shear stress ($\tau_{yz}$) (c) Transverse normal stress ($\sigma_{zz}$)

Figure 7: Through-thickness distribution of normal and shear stresses at $(x, y) = (b/2, L/4)$.

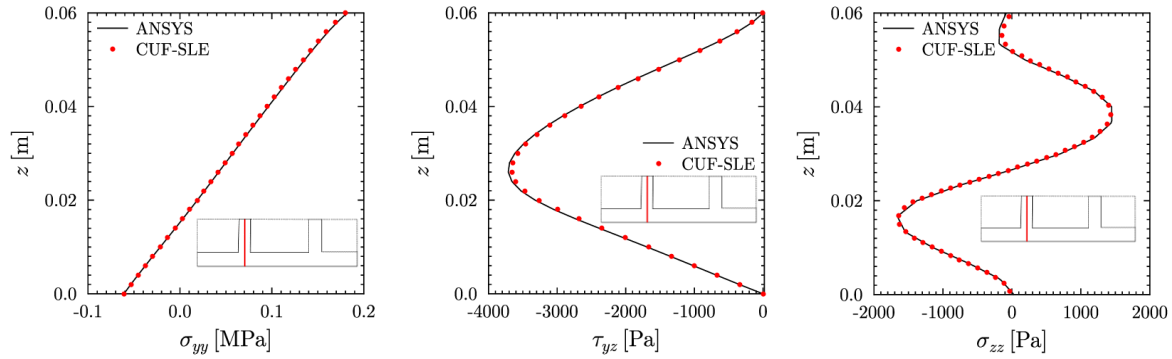


(a) Axial normal stress ($\sigma_{yy}$) (b) Transverse shear stress ($\tau_{yz}$) (c) Transverse normal stress ($\sigma_{zz}$)

Figure 8: Through-thickness distribution of normal and shear stresses at $(x, y) = (b_1 + b_s/2, L/4)$.

### 4.2 Stiffened curved panel

The scope of this section is to assess the proposed higher-order 1D formulation in capturing the structural response of a curved panel, stiffened with stringers and ribs, that usually require the use of 2D or 3D elements. A 3D FE analysis, performed is ANSYS, is used as a reference solution for validation, where the structure is discretised with SOLID186 elements and 9,286,608 equations (DOFs) are solved to yield converged results.

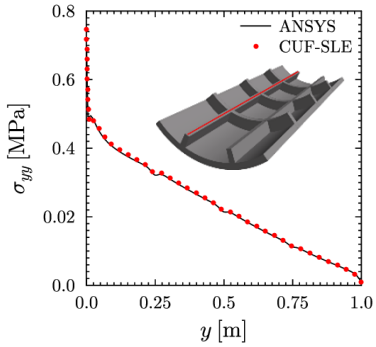


Figure 9: Variation of axial normal stress ($\sigma_{yy}$) along the length of the curved panel.

Figure 9 shows the bending stress distribution at the top of a stringer along its length. Through-thickness variation of axial normal ($\sigma_{yy}$), transverse shear ($\tau_{yz}$) and transverse normal ($\sigma_{zz}$) stresses, computed at the rib-stringer junction at $y = L/4$, is shown in Figure 10. It is to be noted that the results

shown in Figure 10(b) and (c) for $\tau_{yz}$ and $\sigma_{zz}$ are computed in the local coordinate system (obtained by rotating the global coordinate system about *y*-axis such that the *z*-axis point towards the centre of curvature). To highlight the model's ability in capturing localised regions accurately, contour plots of normal and shear stresses ($\sigma_{yy}$ and $\tau_{yz}$) are computed across the entire cross-section at $y = L/4$. The stress distribution obtained using CUF-SLE model is compared with 3D FE results, and the percentage difference is evaluated as shown in Figure 11. From the contour plots, it is evident that the proposed model is capable of predicting an accurate response of the structure with less DOFs than 3D FE.

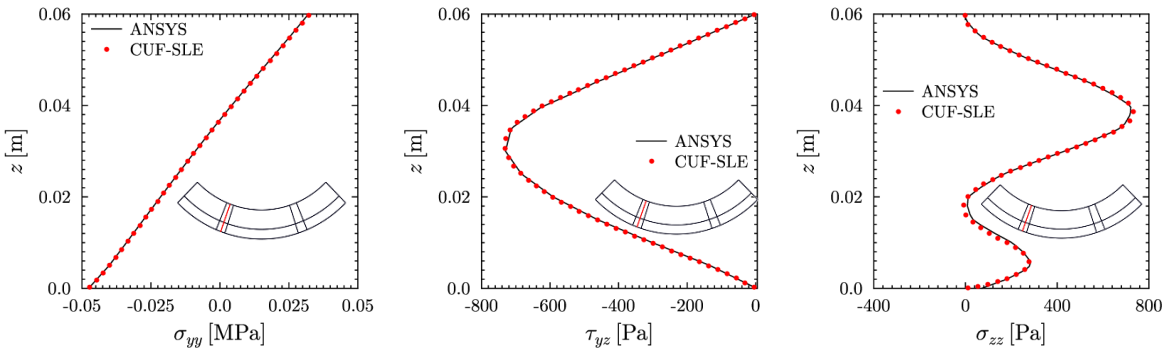


(a) Axial normal stress ($\sigma_{yy}$) (b) Transverse shear stress ($\tau_{yz}$) (c) Transverse normal stress ($\sigma_{zz}$)

Figure 10: Through-thickness distribution of normal and shear stresses at rib-stringer junction ($y = L/4$).

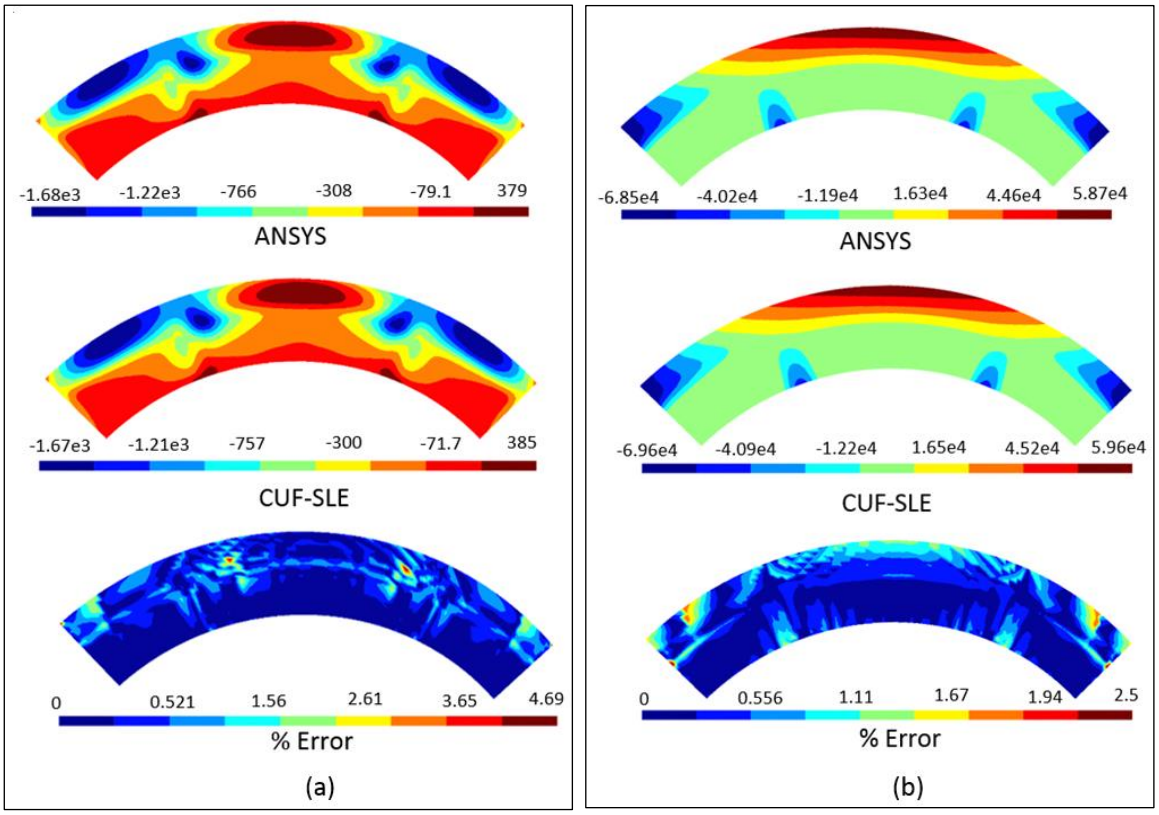


Figure 11: Distribution of (a) normal stress ($\sigma_{yy}$) and (b) shear stress ($\tau_{yz}$) in the cross-section of the curved panel at 25% of the length from the clamped end.

However, it is believed that comparing models based on only DOFs is not a fair assessment of computational efficiency. Instead, computational time must be the criterion for comparison. Although, it could be tricky when comparing in-house codes with a commercial software, as in the present case.

Therefore, we calculate the total number of operations *N*, required to solve the system in both the cases, using the below formula as given in [15], which accounts for the sparsity of a matrix.

$$N = \frac{1}{4} n_{DOFs} (b_w)^2, \tag{11}$$

where $n_{DOFs}$ are the number of unknowns (or DOFs) and $b_w$ is the bandwidth of the stiffness matrix. The number of operations in case of the stiffened curved panel, as calculated using Equation (11), are $N \sim 8.358 \times 10^9$ (3D FE) and $N \sim 3.375 \times 10^9$ (CUF-SLE). This clearly shows that the computation time required to perform a 3D finite element analysis is nearly two and a half times of that required when employing the present formulation. It is to be noted that these numbers are problem dependent and the gain achieved in the computational efficiency over 3D FEA may vary with problems analysed.

## 5 CONCLUSIONS

In the present work, the recently developed Serendipity Lagrange cross-sectional expansion model is employed within the one-dimensional Unified Formulation framework to analyse reinforced structures. The cross-sectional discretisation feature of the SLE model is suited for capturing localised stress fields. It also enables a beam to be modelled with different cross-sections along its length and maintains displacement and stress continuity at the interface. This makes it possible to study complex structures. Moreover, the high-fidelity capabilities of the present model allow 3D stress fields to be modelled accurately and with greater computational efficiency than 3D finite element analysis. Further, the higher-order expansion functions together with the proposed mapping technique and blending functions, enable curved cross-section geometries to be represented. This leads towards the analysis of a broad class of structure regardless of the geometrical complexity of the cross-section. The results of this research provide good confidence for future work to model stiffened structures made of composite materials.

## ACKNOWLEDGEMENTS

This research has been developed in the framework of the FULLCOMP project. The H2020 Marie-Sklodowska Curie European Training Network is gratefully acknowledged.

REFERENCES

[1] O. A. Bauchau and J. I. Craig, Structural Analysis: With Applications to Aerospace Structures, Netherlands: Springer , 2009.

[2] E. J. Sapountzakis and J. T. Katsikadelis, “A new model for slab and beam structures—comparison with other models,” *Computers & Structures,* vol. 80, no. 5-6, pp. 459-470, 2002.

[3] E. Byklum and J. Amdahl, “A simplified method for elastic large deflection analysis of plates and stiffened panels due to local buckling,” *Thin-Walled Structures,* vol. 40, no. 11, pp. 925-953, 2002.

[4] G. Romeo and G. Ferrero, “Analytical/Experimental Behavior of Anisotropic Rectangular,” *AIAA Journal,* vol. 39, no. 5, pp. 932-941, 2001.

[5] A. Pydah and K. Bhaskar, “Accurate discrete modelling of stiffened isotropic and orthotropic rectangular plates,” *Thin-Walled Structures,* vol. 97, pp. 266-278, 2015.

[6] A. Bhar, S. S. Phoenix and S. K. Satsangi, “Finite element analysis of laminated composite stiffened plates using FSDT and HSDT: A comparative perspective,” *Composite Structures,* vol. 92, no. 2, pp. 312-321, 2010.

[7] A. Mukherjee and L. C. Menghani, “Displacement and stress response of laminated beams and stiffened plates using a high-order element,” *Composite Structures,* vol. 28, no. 1, pp. 93-111, 1994.

[8] E. A. Sadek and S. A. Tawfik, "A finite element model for the analysis of stiffened laminated plates," *Computers & Structures,* vol. 75, no. 4, pp. 369-383, 2000.

[9] T. Cavallo, E. Zappino and E. Carrera, "Component-wise vibration analysis of stiffened plates accounting for stiffener modes," *CEAS Aeronautical Journal,* vol. 8, no. 2, pp. 385-412, 2017.

[10] E. Carrera, M. Cinefra, M. Petrolo and E. Zappino, Finite Element Analysis of Structures through Unified Formulation, John Wiley & Sons Ltd, 2014.

[11] E. Carrera and G. Giunta, "Refined beam theories based on a unified formulation," *International Journal of Applied Mechanics,* vol. 02, pp. 117-143, 2010.

[12] S. Minera, M. Patni, E. Carrera, M. Petrolo, P. M. Weaver and A. Pirrera, "Three-dimensional stress analysis for beam-like structures using Serendipity Lagrange shape functions," *International Journal of Solids and Structures,* 2018. doi.org/10.1016/j.ijsolstr.2018.02.030

[13] B. Szabó and I. Babuka, Finite element analysis, London: Wiley, 1991.

[14] A. Pagani, A. d. Miguel and E. Carrera, "Cross-sectional mapping for refined beam elements with applications to shell-like structures," *Computational Mechanics ,* vol. 59, no. 6, pp. 1031-1048, 2017.

[15] J. Thorson, "Gaussian Elimination on a Banded Matrix," *SEP-Report,* vol. 20, pp. 143-154, 1979.